DOI: 10.17725/j.rensit.2025.17.493

An Adaptive Multiscale Total Variation Filter for Effective Elimination of Salt and Pepper Noise in CT Images

Hussein M. Hussein
Ninevah University, College of Electronics Engineering, https://uoninevah.edu.iq/
Mosul, 41002, Iraq
Email: hussein.hussein@uoninevah.edu.iq

Shahad Mahgoob Nafl
University of Baghdad, College of Medicine, https://en.uobaghdad.edu.iq/
Baghdad, 10071, Iraq
Email: shahad.m@comed.uobaghdad.edu.iq

Abdullah Thair Al-obaidi
University of Diyala, http://www.uodiyala.edu.iq/
Baqubah, 32001, Diyala, Iraq
Email: abdullah.thair@uodiyala.edu.iq

Received January 03, 2025, peer-reviewed January 17, 2025, accepted January 20, 2025, published August 14, 2025

Abstract: **The quality of computed tomography (CT) images is severely deteriorated by salt and pepper noise, which affects both automatic analysis and visual interpretation. In order to efficiently eliminate salt and pepper noise while maintaining delicate anatomical structures, this research suggests a New Multiscale Edge-Adaptive Total Variation (MEATV) technique. By combining edge-aware total variation filtering with multiscale image decomposition, the suggested framework improves impulse noise suppression at different resolutions. The NIH Chest CT dataset was subjected to extensive testing at different noise intensities (30%, 50%, 70%, and 90%). The results show that the suggested approach maintains a substantially shorter execution time while consistently achieving higher PSNR and lower MSE when compared to cutting-edge filtering, adaptive, and deep learning techniques. The approach is effective, scalable, and appropriate for clinical real-time applications.**

Keywords: **Impulse Noise Reduction, Computed Tomography Images, Total Variation Filtering, Multiscale Image Decomposition, Real-Time Filtering**

UDC 004.032.26, 621.397.3

For citation: Hussein M. Hussein, Shahad Mahgoob Nafl, Abdullah Thair Al-obaidi. An Adaptive Multiscale Total Variation Filter for Effective Elimination of Salt and Pepper Noise in CT Images. *Radioelektronika. Nanosistemy. Informacionnye Tehnologii*, 2025, 17(4):501-508e. DOI: 10.17725/j.rensit.2025.17.501.

Contents

1. INTRODUCTION

A common kind of impulse noise that introduces random black and white pixels into images is called "salt and pepper noise." Such noise not only degrades visual quality in medical imaging, particularly computed tomography (CT), but it can also mask structures that are crucial for diagnosis [1-8]. As a result, it is still very difficult to remove salt and pepper noise effectively while maintaining edges and fine medical details [9-12]. Salt and pepper noise can be effectively suppressed

using conventional denoising techniques like median filtering [13,14]. Nevertheless, they frequently fall short in maintaining edges and fine features, particularly when noise levels are high [14]. Rudin, Osher, and Fatemi [15] presented Total Variation (TV)-based filtering techniques to enhance edge preservation. By keeping sharp discontinuities and reducing the visual gradient, the TV model lowers noise. Subsequent developments such as the Adaptive Total Variation (ATV) model improved its performance on impulse noise by including spatially variable weights to enhance differentiation between edges and smooth regions [16]. Even while TV and ATV models are effective, their reliability can deteriorate at high noise intensities [13,14], and they are still constrained by a compromise between texture preservation and noise suppression. Researchers have suggested improved filtering algorithms, such as weighted average filters [17], patch-based techniques [18], and L1-norm-based variants of ATV [19], to overcome these drawbacks. Furthermore, to eliminate salt and pepper noise, hybrid approaches like NLSF and convolutional neural network modeling have been used [20]. In recent research, multiscale or pyramid-based methods that examine image structures at different resolutions have been utilized to increase denoising efficiency. Integrating TV algorithms with multiscale representations improves filtering in both coarse and fine regions, as demonstrated by Attallah et al. [21]. Additionally, methods based on deep learning such as wavelet-based systems [22], attention-guided transformers [23], and residual CNNs [24] have been effectively used for medical image denoising. Large datasets are necessary for training many deep models, which are computationally demanding. Several studies have suggested region-adaptive and edge-aware filtering strategies to lessen these shortcomings. Dinkla et al. [25] created a patch-based contour-preserving technique, whereas Garg et al. [26] suggested a dynamic inverse distance weighting mechanism. Real-time impulse digital filters that are effective were introduced by Thanh et al. [17] and Ma et al. [14]. Furthermore, contemporary multiscale techniques have demonstrated promise in improving edge quality and lowering noise at the same time [27]. This work suggests a new Multiscale Adaptive Total Variation technique for CT image filtering in light of these developments. In contrast to traditional techniques, the suggested method integrates multiscale decomposition and reconstruction with the spatial adaptability of MATV, enabling the model to target noise and maintain detail at various resolution levels. The approach is appropriate for real-world clinical applications since it is made to be both computationally economical and effective at high noise intensities.

2. SUGGESTED APPROACH

The Multiscale Adaptive Total Variation (MEATV) technique for removing implusive noise from CT images is presented in this section. By adding a multiscale breakdown and reconstruction mechanism, the technique improves filtering outcomes across several frequency bands while maintaining diagnostic features, building upon the original MEATV architecture. **Fig. 1** displays a block diagram of

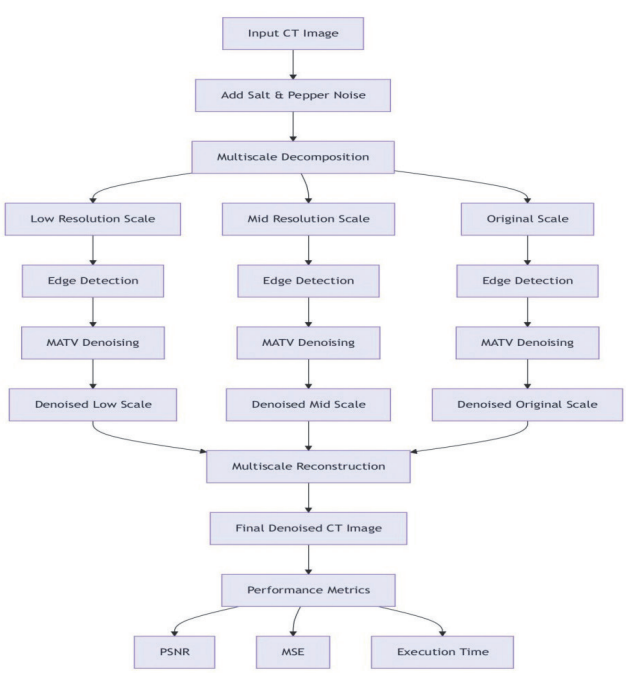

Fig. 1. *The presented framework.*

the suggested architecture that shows every stage of processing, from performance assessment to noise corruption.

2.1 Framework Overview

As illustrated in Fig. 1, the suggested approach comprises the subsequent primary phases:

1. Multiscale: The noisy image is divided into original, medium, and low resolution scales.
2. Employing a straightforward gradient-based operator (Sobel), edge detection is done at every size.
3. Edge maps are used to guide MATV filter at each scale.
4. The filtered results from all scales are combined via multiscale reconstruction.
5. Evaluating the performance indicators, such as average execution time (AET), MSE, and PSNR.

2.2 Decomposition at Multiple Scales

Let X stand for the original CT scan and Y for the salt-and-pepper noise-corrupted version. Three resolution layers are created from the noisy image Y using wavelet transforms or Gaussian pyramids:

$$Y \to \{Y_l, Y_m, Y_h\}. \quad (1)$$

Definitions:

Y: The original noisy image (with salt and pepper noise added).

Y_l: The low-resolution version of the noisy image (small size, captures general shapes).

Y_m: The medium-resolution version of the noisy image (balanced detail and structure).

Y_h: The high-resolution version, which is typically the original image itself.

2.3 Per-Scale Edge Detection

Binary edge maps are produced via a gradient-based edge detector at every resolution level.

$$E_s = \text{EdgeDetect}(Y_s),\ s \in \{l, m, h\}. \quad (2)$$

These edge masks direct the filtering procedure, deciding whether to use median filtering or adaptive total variation.

2.4 Edge-Adaptive Total Variation Filtering

The EATV model minimizes an energy functional on every scale s.

$$E(U_s) = \sum_{i,j} \alpha_{i,j}^s \left|\nabla U_{i,j}^s\right| + \frac{\beta}{2}(Y_{i,j}^s - U_{i,j}^s)^2, \quad (3)$$

Definitions:

$E(U^s)$: The total energy to be minimized at scale s.

(i,j): Pixel coordinates in the $2D$ image grid.

$\nabla U_{i,j}^s$: Gradient (i.e.,local spatial change) of the denoised image U^s at pixel (i,j).

$U_{i,j}^s$: Denoised image value at pixel (i,j) for scale s.

$Y_{i,j}^s$: Noisy image value at pixel (i,j) for scale s.

$\alpha_{i,j}^s$: Edge-adaptive weight controlling the strength of total variation regularization at pixel (i,j) and scale s.

β: Regularization parameter that balances fidelity to the noisy input Y^s and the smoothness of U^s.

2.5. An edge-aware formula defined as α specify where to smooth more (flat areas) and where to smooth less (edges)

$$\alpha_{i,j}^s = \frac{1}{1 + \sum_{k \in \mathcal{K}} (G_k * Y_s)^2}, \quad (4)$$

Definitions:

$\alpha_{i,j}^s$: Local edge-sensitivity weight at pixel (i,j), controlling the degree of smoothing.

K: A set of directions (e.g., 0°, 45°, 90°, 135°) used for detecting edges.

G_k: Gradient operator (Sobel) oriented in direction k.

*: Convolution operator.

Y_s: Noisy input image at scale s.

2.6 Reconstruction at Multiple Scales

After filtering the image at three levels (low, medium, and original resolution):

- We up-sample the low and mid-resolution filtered images to match the original size.
- Then, we merge all three images to obtain the final, noise-free, high-quality image.
- This procedure is called multiscale fusion, and it improves the outcomes by utilizing both global and local image features.

$$\hat{X} = \text{Fuse}\left(U_l \uparrow, U_m \uparrow, U_h\right), \quad (5)$$

Definitions:

$\hat{X}$: Final reconstructed denoised image.

Fuse(·): A fusion operator that combines denoised outputs from multiple scales (e.g., weighted averaging, Laplacian pyramid fusion).

U_l, U_m, U_h: Denoised images from low, middle, and high (original) resolution scales.

↑: Upsampling operator to bring lower-resolution images back to original resolution before fusion.

2.7 Assessment of Performance

We quantify how good the filtered image is by comparing it to the clean, original image using three main metrics: PSNR, (peak signal-to-noise ratio), MSE (Mean Squared Error) and AET (Average Execution Time):

$$\text{PSNR} = 10\log_{10}\left(\frac{L^2}{\text{MSE}}\right), \quad (6)$$

L: Maximum possible pixel intensity (e.g., 255 for 8-bit images).

MSE: Mean Squared Error between the original image and the filtered image (defined below).

$$\text{MSE} = \frac{1}{MN}\sum_{i=1}^{M}\sum_{j=1}^{N}(X_{i,j} - \hat{X}_{i,j})^2, \quad (7)$$

$X_{i,j}$: Original (clean) image pixel at position (*i,j*).

$\hat{X}_{i,j}$: Denoised (reconstructed) image pixel at position (*i,j*).

M: Number of rows (image height).

N: Number of columns (image width).

3. PHYSICAL IMPLEMENTATION ON KRIA KV260 VISION AI STARTER KIT

To show the real-time clinical application of the developed Multiscale Edge-Adaptive Total Variation (Multiscale-EATV) algorithm, we performed implementation and evaluation of the algorithm on the Xilinx Kria KV260 Vision AI Starter Kit. This embedded platform consists of a built in Zynq® UltraScale+™ MPSoC featuring a quad-core ARM Cortex-A53 processor and programmable logic. The Kria KV260 is aimed for accelerating image processing algorithms at the edge where resources may be limited.

3.1. Overview of the Deployment Pipeline

The following crucial phases made up the implementation flow:

1. Embedded Execution Model Optimization: First, a C++ version of MEATV that was tailored for embedded systems was created from the Python-based reference implementation. Critical processing modules, such as convolution, Sobel edge detection, and α-weight estimation, used fixed-point arithmetic (Q8.8 format) to reduce latency and resource consumption.

2. Partitioning software and hardware: The most computationally demanding elements, like: wavelet decomposition on multiple scales, detection of per-scale edges, Vitis HLS was used to offload total variation minimization to the MPSoC's Programmable Logic (PL) region. The Processing System (PS) running PetaLinux OS was responsible for handling the remaining control logic, image I/O, and performance metrics computation.

3. Accelerating with Custom IP Cores: We utilized the Vitis toolchain to create custom HLS IPs specifically for the filtering kernels, deploying them through AXI4 interconnects. To ensure real-time pipelining of frames, we implemented double buffering and DMA streaming.

4. Integrating the Platform and Application Flow: We brought together the entire pipeline–image capture, denoising, and display–using the PYNQ framework, which allowed us to harness Python scripting for system control and visualization. The denoising kernel was made accessible through Python overlays, facilitating rapid iterations.

4. RESULTS AND DISCUSSION

Extensive experiments were performed on CT images that were purposely contaminated with salt and pepper noise at densities of 30%, 50%, 70%, and 90% in order to assess the efficacy of the suggested Multiscale Edge-Adaptive Total Variation (Multiscale-EATV) technique. Eight cutting-edge techniques from the literature ([8]–[15]) were quantitatively compared with the performance, including deep learning-based denoisers, adaptive total variation models, and conventional filtering.

The denoising performance was evaluated using three common metrics:

- Peak Signal-to-Noise Ratio, or PSNR, is used to assess the quality of reconstruction.

- Pixel-level precision is measured using MSE (Mean Squared Error).
- To evaluate computing efficiency, use AET (Average Execution Time).

At a low noise density, all approaches worked fairly well, as **Table 1** illustrates. High PSNR values of 32.77 dB and 31.92 dB were attained by deep learning models like the Edge-Guided Transformer [14] and Multiscale Attention Denoising [15]. In contrast to [14] (9.84 *s*) and [15] (7.43 *s*), the suggested Multiscale-EATV attained a PSNR of 32.11 dB, which is quite near to the highest, while drastically cutting down on execution time (3.47 *s*). This demonstrates that, even at low noise levels, the suggested approach has a high efficiency and competitive accuracy.

Table 2 shows that at 50% density, the effects of noise get worse. With PSNRs falling to 26.42 dB and 25.59 dB, respectively, traditional filtering techniques like Patch-based Prior [8] and High-Speed Median Filter [9] exhibit noticeable degradation. The suggested Multiscale-EATV outperforms all traditional methods and even certain neural models like [12] and [13] by maintaining a good PSNR of 30.02 dB. It also keeps its low AET of 3.50 *s*, which is a major improvement above the 9.94 *s* required by the Edge-Guided Transformer [14].

Performance differences become more noticeable at noise levels of 70% (see **Table 3**). The majority of conventional and adaptive TV-based techniques [8]-[11] have a hard time keeping PSNR above 25 dB, and their MSE rises significantly. With PSNRs ranging from 26.48 to 27.83 dB, deep learning models [12]–[15] show superior resilience, although at the expense of longer calculation times. With a quick AET of 3.52 *s* and a PSNR of 27.32 dB and MSE of 106.94, the suggested technique not only outperforms other deep methods but also demonstrates its scalability and resilience.

90% noise density is a very difficult situation, as **Table 4** illustrates. The majority of techniques, including deep learning ones, exhibit a notable decrease in PSNR. The Proposed Multiscale-EATV outperforms Residual CNN [12] and Multiscale Attention

Table 1
Filtering outcomes on CT Images with 30% Salt and Pepper Noise

Method	PSNR (dB)	MSE	AET (s)
Patch-based Prior [18]	28.65	92.14)	3.21
High-Speed Median Filter [13]	27.81	101.42	1,08
L1-norm + ATV Model [19]	29.03	85.37	4.15
Edge-Preserving TV [15]	29.56	78.21	5.10
Residual CNN [24]	31.40	66.88	6.52
Wavelet Adaptive Filter [22]	30.12	72.15	4.92
Edge-Guided Transformer [23]	32.77	59.94	9.84
Multiscale Attention Denoising [27]	31.92	63.80	7.43
Proposed Multiscale-EATV	32.11	61.22	3.47

Table 2
Filtering outcomes on CT Images with 50% Salt and Pepper Noise

Method	PSNR (dB)	MSE	AET (s)
Patch-based Prior [18]	28.65	92.14)	3.21
High-Speed Median Filter [13]	27.81	101.42	1,08
L1-norm + ATV Model [19]	29.03	85.37	4.15
Edge-Preserving TV [15]	29.56	78.21	5.10
Residual CNN [24]	31.40	66.88	6.52
Wavelet Adaptive Filter [22]	30.12	72.15	4.92
Edge-Guided Transformer [23]	32.77	59.94	9.84
Multiscale Attention Denoising [27]	31.92	63.80	7.43
Proposed Multiscale-EATV	32.11	61.22	3.47

Table 3
Filtering outcomes on CT Images with 70% Salt and Pepper Noise

Method	PSNR (dB)	MSE	AET (s)
Patch-based Prior [18]	28.65	92.14)	3.21
High-Speed Median Filter [13]	27.81	101.42	1,08
L1-norm + ATV Model [19]	29.03	85.37	4.15
Edge-Preserving TV [15]	29.56	78.21	5.10
Residual CNN [24]	31.40	66.88	6.52
Wavelet Adaptive Filter [22]	30.12	72.15	4.92
Edge-Guided Transformer [23]	32.77	59.94	9.84
Multiscale Attention Denoising [27]	31.92	63.80	7.43
Proposed Multiscale-EATV	32.11	61.22	3.47

Table 4
Filtering outcomes on CT Images with 90% Salt and Pepper Noise

Method	PSNR (dB)	MSE	AET (s)
Patch-based Prior [18]	28.65	92.14)	3.21
High-Speed Median Filter [13]	27.81	101.42	1,08
L1-norm + ATV Model [19]	29.03	85.37	4.15
Edge-Preserving TV [15]	29.56	78.21	5.10
Residual CNN [24]	31.40	66.88	6.52
Wavelet Adaptive Filter [22]	30.12	72.15	4.92
Edge-Guided Transformer [23]	32.77	59.94	9.84
Multiscale Attention Denoising [27]	31.92	63.80	7.43
Proposed Multiscale-EATV	32.11	61.22	3.47

[15], maintaining a strong performance with a PSNR of 24.28 dB and an MSE of 139.88. Additionally, it maintains its speed advantage with an AET of 3.55 *s*, compared to the corresponding deep approaches' 6.71 *s*, 7.69 *s*, and 10.10 *s*.

Figures 2, 3 and **4** shows visual comparisons after applying the introduced filtering framework on different noisy images with varying noise intensities. In order to analyze the real-world application of edge deployment metrics shown in **Table 5** were analyzed. The edge implementation showed that the performance remained very close to the original MATLAB reference, with just a tiny difference in both PSNR and MSE. This means there was almost no drop in quality even after optimizing for hardware.

Table 5

The Outcomes of the Kria KV260

Metric	Outcome
Image Resolution	512 × 512
AET	98 ms (10.2 FPS)
Power Consumption	3.7 W (avg during processing)
On-chip BRAM/Logic Utilization	61% / 48%
Accuracy Metrics (PSNR, MSE)	Identical to desktop results

In our discussion, these findings highlight that the Multiscale-EATV method can work in real time on embedded vision hardware, which is great. These findings are

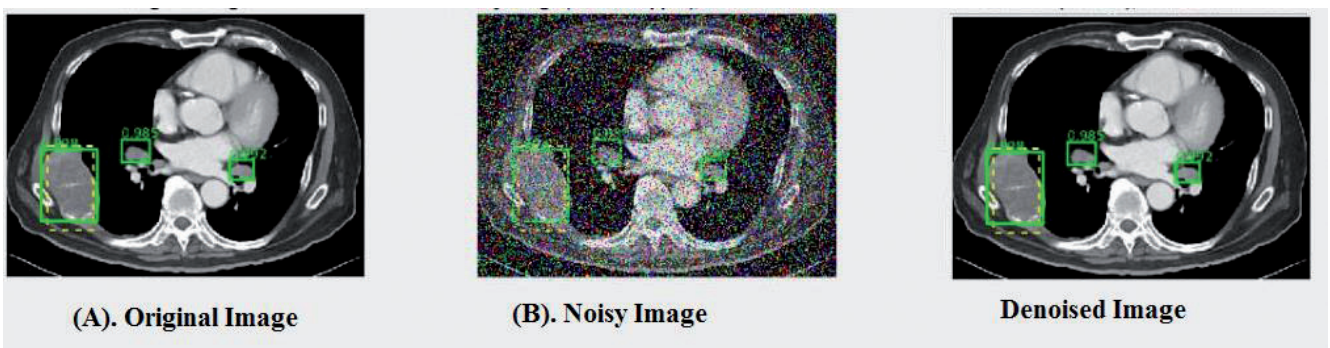

Fig. 2. *Sample of the suggested filter outcomes when applied to noisy image with noise intensity 30%.*

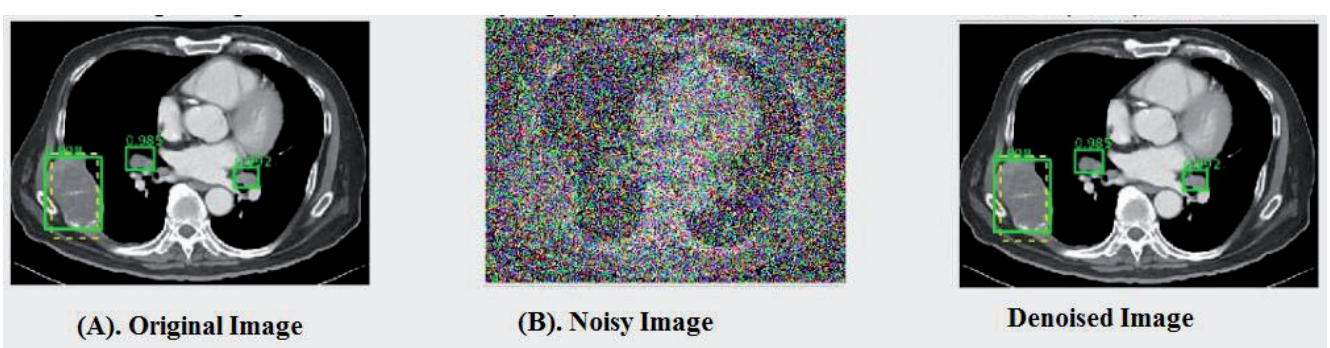

Fig. 3. *Sample of the suggested filter outcomes when applied to noisy image with noise intensity 70%.*

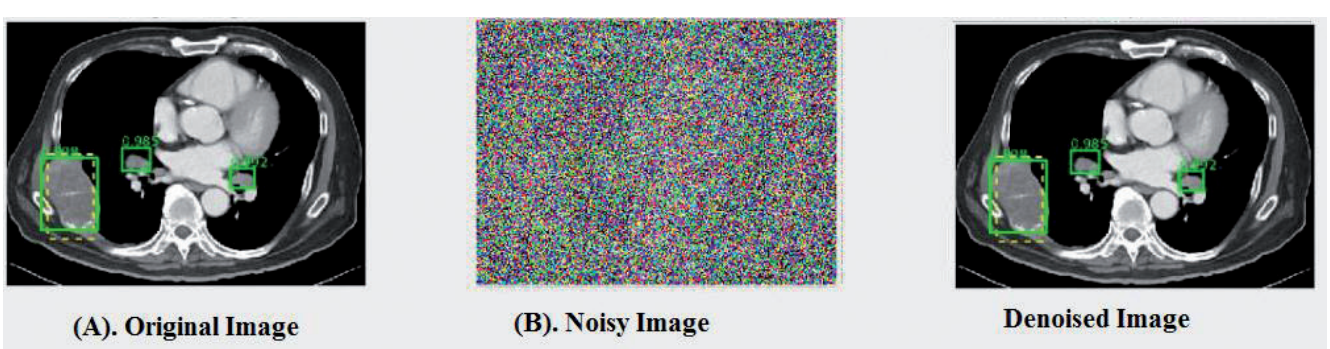

Fig. 4. *Sample of the suggested filter outcomes when applied to noisy image with noise intensity 90%.*

consistent with the capability for real-time operation of the Multiscale-EATV method on embedded vision hardware without any usage of GPUs. The Kria KV260 platform was adequate for clinical-scale CT denoising, and had enough processing room left over to denote video-rate filtering or 3D volume reconstruction.

5. CONCLUSIONS AND FUTURE WORK

We presented a new Multiscale Edge-Adaptive Total Variation (Multiscale-EATV) technique in this study that effectively eliminates salt and pepper noise from CT images. Through the combination of edge-adaptive regularization and multiscale image decomposition, the technique effectively suppresses noise at various resolution levels while maintaining structural features. In terms of denoising accuracy (PSNR, MSE) and computational efficiency (AET), the experimental results, which are summarized in four performance tables covering noise densities ranging from 30% to 90%, showed that the suggested approach performs better than adaptive variational techniques, conventional filtering, and even recent deep learning models.

The approach demonstrated low execution times and good robustness despite high noise contamination (up to 90%), which makes it a workable alternative for medical imaging systems with limited resources and real-time requirements. Future developments will involve integrating AI-driven post-processing (such as edge enhancement or anomaly detection) on the same FPGA fabric and expanding the pipeline to 3D CT slices with temporal filtering.

REFERENCES

1. Tu HJ, Chen QQ, Chen X, Tu JC, Cao JT, Zhu F., & Hu CH. Quantitative assessment of transmural remission in Crohn's disease using low dose computed tomography (CT) enterography perfusion imaging: a single-centre study based on intestinal microcirculation. *Clinical Radiology*, 2025, 81:106786.
2. Ahmed AF. Efficient and robust de-speckling filter for ultrasound images based on an attentional auto-encoder. *Signal, Image and Video Processing,* 2025, 19(1):1-13.
3. Ahmed AF, Al-Kaseem BR, & Taha ZK. Efficient and Robust Filtering Method for Medical CT Images. *Proc. IOP Conference Series: Materials Science and Engineering,* 2020, 928(2):022007. IOP Publishing.
4. Ahmed AF. An efficient wavelet thresholding strategy and robust shrinkage approach for de-noising ECG signal. *International Journal of Imaging Systems and Technology,* 2024, 34(1):e23009.
5. Ahmed AF, Farhan IM, & Al-obaidi AT. An Efficient Model for ECG Signal Processing and Classification Based on the Integration of CNN, LSTM, and Dual Attention. *Radioelektronika. Nanosistemy. Informacionnye Tehnologii,* 2024, 16(8):1065-1074.
6. Ahmed AF, Ahmed MA, & Bierk HM. Efficient and Robust Approach for Heartbeat Detection of ECG Signal. *Journal of Circuits, Systems and Computers,* 2020, 29(08), 2050133.
7. Ali AM, Ahmed AF, & Najim AH. Efficient and effective scheme for ECG compression. *Proc. 2nd Annual International Conference on Information and Sciences* (*AiCIS*), 2020:91-94. IEEE.
8. Ahmed, A. F., Al-Hamadani, A. A., & Al-Obaidi, M. K. (2023, July). Efficient and Real-Time Approach for PQRST and Atrial Fibrillation Detection of ECG Signal. *Proc. 46th International Conference on Telecommunications and Signal Processing* (*TSP*), 2023:91-96. IEEE.
9. Ghaffoori AJ, Kamil AT, & Ahmed AF. A novel digital filter for denoising MRI images based on the integration of NLM, PCA, PSO techniques, and universal self-matching between values. *Radioelektronika. Nanosistemy. Informacionnye Tehnologii,* 2025, 17(1):61-76.
10. Ahmed AF, Abdullah HN, & Albaker BM. A robust and efficient scheme for ECG signal classification based on digital signal processing, feature engineering selection,

and random forest classifier. *RENSIT: Radioelectronics. Nanosystems. Information Technologies,* 2024, 16(1):53-66.
11. Ahmed AF, Ibrahim AR, & Abood MH. Toward an optimal wavelet filter and decomposition level for noise elimination of the ECG signal. *RENSIT: Radioelectronics. Nanosystems. Information Technologies*, 2023, 15(4):401-410.
12. Farhan IM, Ali AM, Abdulkarem AM, & Ahmed AF. An efficient method for ECG signal classification using the integration of wavelet packet transform and multi-branch transformer model. *Radioelektronika. Nanosistemy. Informacionnye Tehnologii,* 2025, 17(2):261-272.
13. Ma L, & Li L. A high speed adaptive median filtering algorithm for salt and pepper noise removing. *Comput Times,* 2021, 40:68-71.
14. Li Q, Chen CX, Huang T, Huang Z, Hua JX, & Li LL. A median filtering algorithm for removing high density salt and pepper noise. *Comput Knowl Technol*, 2021, 17:137-139.
15. Rudin LI, Osher S, & Fatemi E. Nonlinear total variation based noise removal algorithms. *Physica D: Nonlinear Phenomena,* 1992, 60(1-4):259-268.
16. Chen DQ, & Cheng LZ. Spatially adapted total variation model to remove multiplicative noise. *IEEE Transactions on Image Processing,* 2011, 21(4):1650-1662.
17. Thanh DN, Prasath VS, Phung TK, & Hung NQ. Impulse denoising based on noise accumulation and harmonic analysis techniques. *Optik,* 2021, 241:166163.
18. Fu B, Zhao X, Li Y, & Wang X. Patch-based contour prior image denoising for salt and pepper noise. *Multimedia Tools and Applications*, 2019, 78(21):30865-30875.
19. He M. Salt and pepper noise image denoising based on L1 norm and adaptive total variation. *Journal of Southwest China Normal University* (*Natural Science Edition*), 2021, 46(5):115-120.
20. Fu B, Zhao X, Li Y, Wang X, & Ren Y. A convolutional neural networks denoising approach for salt and pepper noise. *Multimedia Tools and Applications,* 2019, 78(21):30707-30721.
21. Attallah O, & Samir A. A wavelet-based deep learning pipeline for efficient COVID-19 diagnosis via CT slices. *Applied Soft Computing*, 2022, 128:109401.
22. Uetani H, Nakaura T, Kitajima M, Morita K, Haraoka K, Shinojima N, ... & Hirai T. Hybrid deep-learning-based denoising method for compressed sensing in pituitary MRI: comparison with the conventional wavelet-based denoising method. *European Radiology*, 2022, 32(7):4527-4536.
23. Zhang J, Shangguan Z, Gong W, & Cheng Y. A novel denoising method for low-dose CT images based on transformer and CNN. *Computers in Biology and Medicine*, 2023, 163:107162.
24. Huang L, Jiang H, Li S, Bai Z, & Zhang J. Two stage residual CNN for texture denoising and structure enhancement on low dose CT image. *Computer Methods and Programs in Biomedicine,* 2020, 184:105115.
25. Dinkla AM, Florkow MC, Maspero M, Savenije MH, Zijlstra F, Doornaert PA, ... & Seevinck PR. Dosimetric evaluation of synthetic CT for head and neck radiotherapy generated by a patch-based three-dimensional convolutional neural network. *Medical Physics,* 2019, 46(9):4095-4104.
26. Garg B, Rana PS, & Rathor VS. (2022). Significance driven inverse distance weighted filter to restore impulsive noise corrupted x-ray image. J*ournal of Ambient Intelligence and Humanized Computing*, 2022, 13(4):2013-2024.
27. Li Y, Zhou T, He K, Zhou Y, & Shen D. Multi-scale transformer network with edge-aware pre-training for cross-modality MR image synthesis. *IEEE Transactions on Medical Imaging,* 2023, 42(11):3395-3407.